J Physiol 591.14 (2013) pp 3539–3548

The Journal of Physiology

Effects of the insertional and appositional forces of the canine diaphragm on the lower ribs

Theodore A. Wilson[1] and André De Troyer[2,3]

[1] *Department of Aerospace Engineering and Mechanics, University of Minnesota, Minneapolis, MN 55455, USA*
[2] *Laboratory of Cardiorespiratory Physiology, Brussels School of Medicine, 1070 Brussels, Belgium*
[3] *Chest Service, Erasme University Hospital, 1070 Brussels, Belgium*

Key points

- Although the diaphragm causes a fall in pleural pressure, it expands the lower portion of the ribcage when it contracts.
- This action is conventionally considered to be the result of two mechanisms, namely, the force applied by the muscle fibres on the ribs into which they insert (insertional force) and the transmission of abdominal pressure through the zone of apposition (appositional force).
- In this study in anaesthetized dogs, we assessed the magnitude of the force exerted by the diaphragm on the lower ribs and the relative contributions of the insertional and appositional components.
- The results show that, per unit pressure, the inspiratory effect of the diaphragmatic force on the lower ribs is equal to the expiratory effect of pleural pressure and that the insertional force contributes 60% of that inspiratory effect.

Abstract The diaphragm has an inspiratory action on the lower ribs, and current conventional wisdom maintains that this action is the result of two mechanisms, namely, the force applied by the muscle fibres on the ribs into which they insert (insertional force) and the transmission of abdominal pressure through the zone of apposition (appositional force). The magnitude of the diaphragmatic force and the relative contributions of the insertional and appositional components, however, are unknown. To assess these forces, the inspiratory intercostal muscles in all interspaces were severed in anaesthetized dogs, so that the diaphragm was the only muscle active during inspiration, and the displacements of the lower ribs along the craniocaudal and laterolateral axes were measured during quiet breathing, during occluded breaths and during passive lung inflation. From these data, the isolated effects of pleural pressure and transdiaphragmatic pressure on rib displacement were determined. Then external forces were applied to the ribs in the cranial and the lateral direction to simulate, respectively, the effects of the insertional and appositional forces, and the rib trajectories for these external forces were used as the basis for a vector analysis to obtain the relative magnitudes of the insertional and appositional contributions to the rib displacement driven by transdiaphragmatic pressure. The results show that, per unit pressure, the inspiratory effect of the diaphragmatic force on the lower ribs is equal to the expiratory effect of pleural pressure, and that the insertional force contributes 60% of that inspiratory effect.

(Received 11 February 2013; accepted after revision 1 May 2013; first published online 27 May 2013)
Corresponding author A. De Troyer: Chest Service, Erasme University Hospital, Route de Lennik, 808, 1070 Brussels, Belgium. Email: a_detroyer@yahoo.fr

Abbreviations P_{ab}, abdominal pressure; P_{di}, transdiaphragmatic pressure; P_{eff}, effective total pressure; P_{pl}, pleural pressure.

DOI: 10.1113/jphysiol.2013.253286

Introduction

Measurements of thoracoabdominal motion in subjects with quadriplegia due to complete, traumatic transaction of the cervical cord (Mortola & Sant'Ambrogio, 1978; Danon *et al.* 1979; Strohl *et al.* 1984; Estenne & De Troyer, 1985; Urmey *et al.* 1986) and studies of rib displacements in dogs (De Troyer, 2011, 2012) have established that isolated contraction of the diaphragm during breathing produces an inward displacement of the upper portion of the ribcage and an expansion of the lower portion of the ribcage. The expiratory action of the diaphragm on the upper ribs is primarily caused by the fall in pleural pressure, and current conventional wisdom maintains that the inspiratory action on the lower ribs is the result of two components of the force developed by the muscle (De Troyer & Boriek, 2011). The first component, denoted the 'insertional force', is the direct cranial force applied by the muscle fibres of the costal portion of the diaphragm on the ribs into which they insert. The second component, the 'appositional force', is the lateral force due to the transmission of abdominal pressure to the lower ribcage in the zone of apposition (Mead, 1979).

Loring & Mead (1982) presented a model for the forces exerted by the diaphragm on the ribcage. They described the effective total pressure acting on the ribcage during diaphragmatic contraction (P_{eff}) as the sum of pleural pressure (P_{pl}) and the effect of the forces exerted by the muscle, which are proportional to transdiaphragmatic pressure (P_{di}), as follows:

$$P_{eff} = P_{pl} + B \times P_{di} \quad (1)$$

From their modelling, they estimated that the coefficient of proportionality $B = 0.65$ and that the insertional force contributed ~25% of the value of B and the appositional force contributed ~75%. These estimates, however, have never been tested experimentally.

The objective of the present study was to measure the magnitudes of the contributions of the forces exerted by the diaphragm to the displacement of the lower ribs. The inspiratory intercostal muscles were severed in all interspaces in dogs, so that the diaphragm was the only muscle active during inspiration, and the displacements of the lower ribs along the craniocaudal and laterolateral axes of the body were measured during quiet, unimpeded breathing, during single inspiratory efforts against an occluded airway and during passive lung inflation. From these data, the effects of P_{pl} and P_{di} on rib displacement were determined. Then, external forces were applied to the ribs in the cranial and lateral directions to simulate the effects of the insertional and appositional forces, respectively. The rib trajectories for these external forces were used as the basis for a vector analysis to obtain the relative magnitudes of the insertional and appositional contributions to the rib displacement driven by P_{di}. The results support the concept of insertional and appositional components of the force exerted by the diaphragm on the lower ribs, but they show that the magnitudes of the effects of these components are quite different from those estimated by Loring & Mead (1982).

Methods

The studies were carried out on eight adult bred-for-research dogs (22–30 kg) anaesthetized with pentobarbital sodium (initial dose, 30 mg kg^{-1} I.V.), as approved by the Animal Ethics and Welfare Committee of the Brussels School of Medicine. The animals were placed in the supine position and intubated with a cuffed endotracheal tube, and a venous cannula was inserted in the forelimb to give maintenance doses of anaesthetic (3–5 mg kg^{-1} h^{-1} I.V.). The abdomen was opened by a 4-cm-long mid-line incision cranial to the umbilicus, and a balloon-catheter system filled with 1.0 ml of air was placed between the stomach and the liver and connected to a differential pressure transducer (Validyne, Northridge, CA, USA) to measure the change in abdominal pressure (ΔP_{ab}). After the abdomen was closely sutured, the ribcage and intercostal muscles were exposed on both sides of the chest from the first to 11th rib by reflection of the skin and superficial muscle layers, and the inspiratory intercostal muscles were eliminated from the act of breathing using the same method that has been described previously in detail (De Troyer, 2011, 2012). Thus, the external intercostal muscles in interspaces one to eight were severed bilaterally from the chondrocostal junctions to the spine, and the internal intercostal nerves in interspaces two to eight on the right side and in interspaces three to eight on the left side were sectioned at the chondrocostal junctions to denervate the corresponding parasternal intercostal muscles. The parasternal intercostal muscle in the first interspace was also sectioned bilaterally from the sternum to the chondrocostal junction. Denervation of the parasternal intercostal in each interspace was demonstrated by the suppression of the inspiratory EMG activity, and postmortem examination of the thorax confirmed that the external intercostal and levator costae muscles in all interspaces were entirely severed. Finally two hooks were implanted in the 10th rib pair near the midaxillary line, i.e. in one of the rib pairs into which the diaphragm inserts in the dog (Evans & Christensen, 1979), so that the ribs could be manipulated later.

Measurements

After completion of the surgical procedure, an additional hook was screwed in the right 10th rib in the midaxillary line, and the hook was connected by long, inextensible threads to two linear displacement transducers (Schaevitz Engineering, Pennsauken, NJ, USA) to measure rib displacement along both the craniocaudal

(axial) and the laterolateral axes. This technique has been previously described in detail (De Troyer & Kelly, 1982; De Troyer & Wilson, 2000). In addition, a balloon-catheter system filled with 0.5 ml of air was placed in the mid-oesophagus to measure the changes in pleural pressure (ΔP_{pl}), and a pair of silver hook electrodes spaced 3–4 mm apart was inserted in the intact parasternal intercostal muscle of the second left interspace to provide a time reference for pressure and rib displacement and to quantify neural inspiratory drive. The position of the oesophageal balloon was adjusted by the occlusion technique (Baydur *et al.* 1982), and the parasternal electrodes were implanted in parallel fibres in the muscle area known to receive the greatest inspiratory drive, i.e. in the vicinity of the sternum (De Troyer *et al.* 2005). The EMG signal was processed with an amplifier (model 830/1; CWE, Ardmore, PA, USA), bandpass filtered from 100 to 2000 Hz, and rectified before its passage through a leaky integrator with a time constant of 0.2 s.

Protocol

Baseline parameters were allowed to stabilize for 30 min following completion of the surgical instrumentation, after which measurements of rib displacement, ΔP_{pl}, ΔP_{ab} and parasternal intercostal EMG activity were obtained. The animal was breathing spontaneously throughout. Every 10–15 breaths, however, the endotracheal tube was occluded at end expiration for a single inspiratory effort. Five to six occluded breaths were recorded in each animal. After completion of these measurements, the animal was connected to a mechanical ventilator (Harvard Apparatus, Holliston, MA, USA) and hyperventilated until the disappearance of the parasternal intercostal EMG activity.

Inextensible threads were then connected to the hooks implanted in the 10th rib on both sides of the chest, and the animal was disconnected from the ventilator. The threads were pulled first in the direction perpendicular to the sagittal mid-plane of the body so as to simulate the action of P_{ab} on the rib. The pulling was made gradually until the rib lateral displacement was ∼4–5 mm. Three trials were performed in each animal. The 10th rib pair was then pulled in the cranial–dorsal direction to simulate the direct force applied on the lower ribs by the muscle fibres of the costal portion of the diaphragm. Recent studies using computed tomography (Leduc *et al.* 2012; De Troyer *et al.* 2012) have shown that in supine dogs at functional residual capacity, these muscle fibres make an acute angle of 24.9 ± 1.7 deg (mean ± SEM) relative to the craniocaudal axis of the body. In order to reproduce as closely as possible the effect of the insertional force of the diaphragm, therefore, a protractor was laid near the rib hook, and while the animal was still apnoeic at functional residual capacity, the 10th rib pair was gradually pulled along a direction that made a 25 deg angle relative to the horizontal plane. The procedure was performed in triplicate in each animal.

The animals were maintained at a constant, rather deep level of anaesthesia throughout the study. They had no pupillary light reflex and made no spontaneous movements other than respiratory movements both during the surgery and during the measurements. The corneal reflex was also abolished during the surgery. Rectal temperature was maintained constant between 36 and 38°C with infrared lamps. At the end of the experiment, the animals were killed with pentobarbital sodium (30–40 mg kg^{-1} I.V.).

Data analysis

The analysis of the data for each animal was made in four stages. First, the peak inspiratory displacement of rib 10 along the craniocaudal axis (X) and the laterolateral axis (Y) and ΔP_{ab} and ΔP_{pl} during spontaneous diaphragmatic breathing were averaged over five consecutive breaths, and the changes in trans-diaphragmatic pressure (ΔP_{di}) were calculated ($\Delta P_{di} = \Delta P_{ab} - \Delta P_{pl}$). The rib displacements and pressure changes recorded during occluded breaths and during mechanical, passive lung inflation were analysed in a similar manner. It should be pointed out that the values of rib displacement and pressure changes during unimpeded breaths and during occluded breaths were measured relative to the onset of the inspiratory burst in the parasternal intercostal of the second left interspace. The values that were considered in the data analysis, therefore, resulted exclusively from the contraction of the diaphragm (and the single parasternal intercostal of the second left interspace) and were not corrupted by the relaxation of the abdominal muscles and the internal interosseous intercostals at the end of expiration. By convention, positive rib displacements indicate inspiratory displacements in the cranial or outward direction.

In the second stage, the rib trajectory driven by ΔP_{di} alone was determined by using the following equations, where the coefficients a and c describe, respectively, the craniocaudal and laterolateral rib displacement produced by a unit change in ΔP_{pl} alone, and the coefficients b and d describe the craniocaudal and laterolateral rib displacement produced by a unit change in ΔP_{di} alone:

$$X = a\Delta P_{pl} + b\Delta P_{di} \quad (2)$$

$$Y = c\Delta P_{pl} + d\Delta P_{di} \quad (3)$$

The values of these coefficients were obtained by finding the values that gave the best fit of the equations to the values of rib displacement and pressure changes measured during the three manoeuvres (namely, unimpeded breaths, occluded breaths and mechanical ventilation).

In the third stage, the rib trajectories induced by the application of external forces to the rib were determined. Thus, for each pull of the 10th rib pair in the lateral direction and the cranial–dorsal direction, the lateral rib displacement (Y) was measured at 0.3–0.7 mm increments of cranial displacement (X), and the values were averaged over the three trials. The values of Y were then plotted against the values of X, and straight lines were fitted to the data. As illustrated by the data obtained in a representative animal in Fig. 1, straight lines fitted the data very well in every animal (coefficient of correlation, r between 0.999 and 1.0), but in many animals the lines of best fit did not pass through the origin. Instead, the lines had a small positive Y intercept; for the animal group, the intercept during pulling in the lateral direction was 0.16 ± 0.03 mm and that during pulling in the cranial–dorsal direction was 0.11 ± 0.03 mm. These intercepts were considered to be artifacts, due to the fact that the external forces were applied at a single point on one rib, rather than being distributed around the circumference of the ribcage. These intercepts, therefore, were ignored, and their values were subtracted from the values of lateral rib displacement so that the relationships passed through the origin.

In the final stage, the rib trajectory driven by ΔP_{di} was compared with the trajectories induced by external forces, and the axial and lateral components of the effect of ΔP_{di} were determined by using a vector analysis, as shown in Fig. 2. The line O–Q in the figure corresponds to the rib trajectory driven by ΔP_{di} alone during spontaneous, unimpeded diaphragmatic breathing, while the dashed lines are the trajectories driven by the external lateral and cranial–dorsal forces, and the lines O–L and O–A are the vectors along the external force trajectories that are the components of the resultant O–Q. The component O–A projected onto the resultant is the segment O–P. The ratio of the length of this segment to the length O–Q, therefore, is the fraction of the rib displacement contributed by the insertional force of the diaphragm, and the ratio of the length of the segment P–Q to the length O–Q is the fraction of the rib displacement contributed by the appositional force.

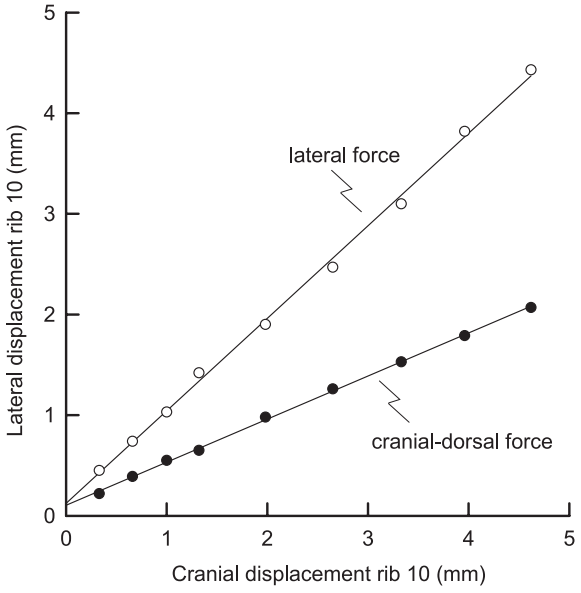

Figure 1. Trajectory of rib 10 during the application of external forces to the rib
The data points were obtained in a representative animal while the animal was made apnoeic by mechanical hyperventilation and the 10th rib pair was pulled in the lateral (open circles) and the cranial–dorsal direction (filled circles). The lines of best fit to the data are also shown. The lines did not pass through the origin, and the small positive intercepts with the ordinate were considered to be artifacts.

Results

Baseline data

The records of P_{pl}, P_{ab}, rib 10 displacement and parasternal intercostal EMG activity in the second left

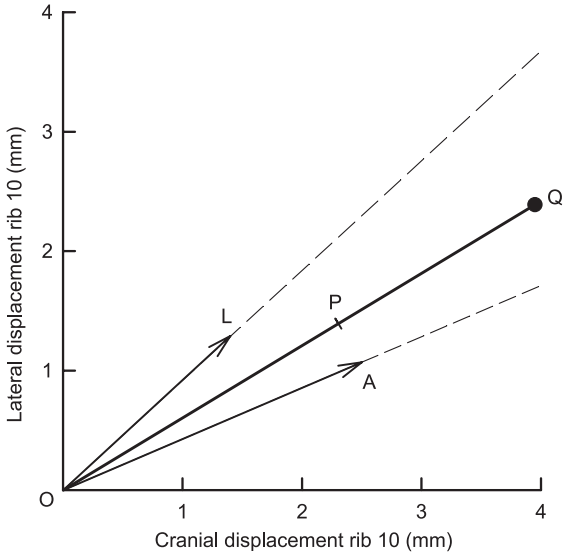

Figure 2. Comparison between the trajectory of rib 10 during spontaneous breathing and the trajectories during the application of external forces
Data are from the same animal as in Fig. 1. The continuous line O–Q corresponds to the rib trajectory driven by transdiaphragmatic pressure (ΔP_{di}) alone for $P_{di} = 5$ cmH_2O, and the dashed lines correspond to the rib trajectories obtained during the application of external forces to the rib in the lateral and cranial–dorsal directions. These two trajectories are the relationships shown in Fig. 1 but transposed so as to pass through the origin. The lines O–A and O–L are the vectors along these trajectories that are the components of the resultant O–Q, and the point P was defined by drawing through point A the normal to O–Q. The segment O–P, therefore, was taken as the rib displacement contributed by the insertional force, and the segment P–Q was taken as the displacement contributed by the appositional force.

interspace obtained in a representative animal during three unimpeded breaths and an occluded breath performed with the diaphragm alone and during mechanical ventilation are shown in Fig. 3, and the mean ± SEM values of inspiratory rib displacement, ΔP_{pl} and ΔP_{di} obtained from the eight animals in the three manoeuvres are listed in Table 1. During unimpeded breaths, rib 10 moved cranially and outward during the inspiratory phase of the breathing cycle in all animals. For the eight animals, the displacement of the rib in the cranial and outward direction at peak inspiration was 1.20 ± 0.24 and 0.88 ± 0.18 mm, respectively. The rib also moved cranially and outward during occluded breaths in seven of eight animals and during mechanical ventilation in all animals.

Rib displacement driven by ΔP_{di}

The values of the coefficients *a*, *b*, *c* and *d* computed in the eight animals are listed in Table 2. The values of *a* and *b* were nearly equal, and the values of *c* and *d* were also nearly equal. However, the values of *a* and *b* were consistently greater than the values of *c* and *d*. Also, as shown in Fig. 4, the value of the ratio *a*/*c* was nearly equal to the value of the ratio *b*/*d* in every animal, and this implies that the *X*–*Y* trajectories of the rib driven by ΔP_{pl} alone and ΔP_{di} alone were the same. This is shown for spontaneous, unimpeded diaphragmatic breathing in Fig. 5. The filled circle in the figure (point E) corresponds to the mean ± SEM rib displacement measured in the eight animals, and the open circle (point G) represents the position of the rib that would have occurred if ΔP_{di} were zero. The dashed line O–G, therefore, is the rib displacement due to ΔP_{pl} alone, and the continuous line G–E is the rib displacement produced by ΔP_{di}. These two displacements are clearly superimposed. The figure also shows that, although the measured displacement of the rib during diaphragmatic breathing, defined by the length of the segment O–E, was only 1.5 ± 0.3 mm, the rib displacement due to ΔP_{di} was much larger and averaged 5.3 ± 0.7 mm.

The contributions of ΔP_{pl} and ΔP_{di} to the total rib displacement were also obtained from the values of the coefficients in eqns (2) and (3). Total rib displacement, denoted *Z*, is given by eqn (4), as follows:

$$Z = \sqrt{X^2 + Y^2} \tag{4}$$

Substituting for *X* and *Y* from eqns (2) and (3) in eqn (4) yields a complicated relationship between *Z* and ΔP_{pl} and ΔP_{di}. However, because the value of *a*/*c* in every animal was nearly equal to the value of *b*/*d* (Fig. 4), eqn (4) simplifies to the following:

$$Z = A \times (\Delta P_{pl} + C\Delta P_{di}) \tag{5}$$

$$A = \sqrt{a^2 + c^2} \quad C = b/a$$

Thus, the coefficient *A* in eqn (5) describes the total rib displacement driven by a unit ΔP_{pl}, and the coefficient *C* describes the effect of a unit ΔP_{di} on the total rib displacement relative to the effect of ΔP_{pl}. For the animal group, *A* was 0.86 ± 0.09 mm cmH_2O^{-1}, and *C* was 0.98 ± 0.06.

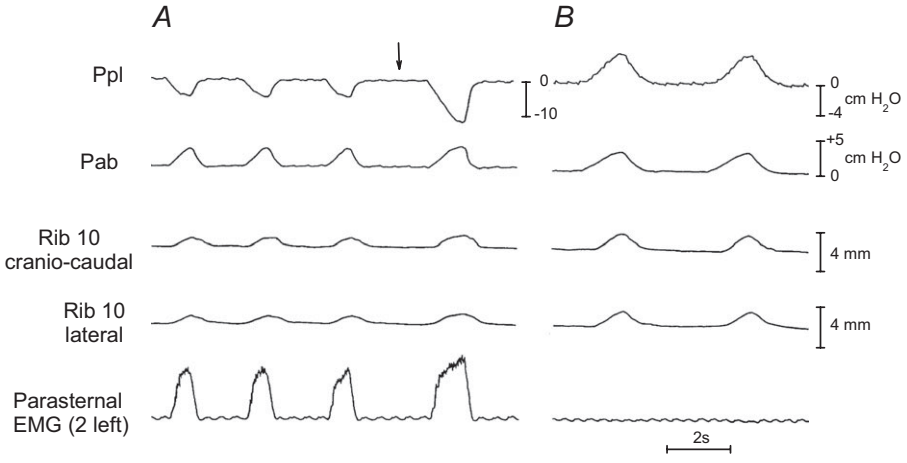

Figure 3. Records of rib 10 displacement and pressure changes during isolated, spontaneous contraction of the diaphragm (*A*) and during mechanical ventilation (*B*) in a representative animal
The external intercostal muscles in all interspaces were severed, and all the parasternal intercostal muscles but the one in the second left interspace were denervated or severed. The diaphragm, therefore, was the only muscle active during inspiration, and the trace of EMG activity (integrated signal) in the parasternal intercostal in the second left interspace provided the time reference. The traces of pleural (P_{pl}) and abdominal pressure (P_{ab}) are also shown. The rib moved cranially and outward (upward deflections) both during unimpeded inspiration and during single occluded breaths (breath after arrow in *A*); they also moved cranially and outward during mechanical, passive lung inflation (*B*).

Table 1. Displacement of rib 10 and pressure changes during spontaneous diaphragmatic breathing and mechanical ventilation in dogs

	Axial rib motion (mm)	Lateral rib motion (mm)	ΔP_{pl} (cmH_2O)	ΔP_{ab} (cmH_2O)	ΔP_{di} (cmH_2O)
Quiet breathing	1.20 ± 0.24	0.88 ± 0.18	-4.46 ± 0.47	$+2.24 \pm 0.36$	$+6.71 \pm 0.77$
Occluded breaths	1.26 ± 0.34	1.00 ± 0.22	-12.57 ± 1.14	$+2.23 \pm 0.35$	$+14.80 \pm 1.35$
Mechanical ventilation	1.83 ± 0.20	1.16 ± 0.19	$+4.93 \pm 0.18$	$+2.44 \pm 0.23$	-2.50 ± 0.26

Values are means $\pm$ SEM for eight dogs. Abbreviations: P_{ab}, abdominal pressure; P_{di}, transdiaphragmatic pressure; and P_{pl}, pleural pressure.

Table 2. Rib displacements produced by unit changes in pleural and transdiaphragmatic pressure in eight dogs

Dog no.	a (mm cmH_2O^{-1})	b (mm cmH_2O^{-1})	c (mm cmH_2O^{-1})	d (mm cmH_2O^{-1})
Dog 1	0.55	0.73	0.29	0.39
Dog 2	0.76	0.81	0.42	0.49
Dog 3	1.12	1.10	0.61	0.63
Dog 4	0.64	0.57	0.48	0.44
Dog 5	0.47	0.45	0.42	0.40
Dog 6	0.97	0.91	0.76	0.73
Dog 7	0.66	0.53	0.49	0.39
Dog 8	0.60	0.53	0.27	0.27
Mean	0.72	0.70	0.47	0.47
SEM	0.08	0.08	0.06	0.05

Note that a and b are the coefficients in the equation $X = a\Delta P_{pl} + b\Delta P_{di}$, where X is the axial displacement of rib 10 in millimetres, ΔP_{pl} is the change in pleural pressure in centimetres of water, and ΔP_{di} is the change in transdiaphragmatic pressure in centimetres of water. Note also that c and d are the coefficients in the equation $Y = c\Delta P_{pl} + d\Delta P_{di}$, where Y is the laterolateral displacement of rib 10 in millimetres.

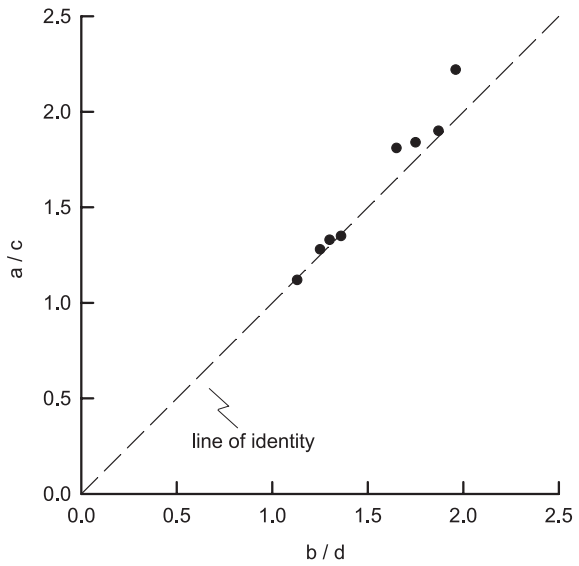

Figure 4. Relationship between the coefficients of rib displacement in eight dogs
The values of the ratio *b/d* obtained in the eight animals are shown on the abscissa, and the corresponding values of the ratio *a/c* are shown on the ordinate. The dashed line is the line of identity. All the individual values were close to the identity line, implying that during breathing the rib always moves along a single trajectory.

Rib trajectories produced by external forces

When the 10th rib pair was pulled in the lateral direction, rib 10 moved outward and cranially. The rib also moved both cranially and outward when the rib pair was pulled in the cranial–dorsal direction. As shown by the records of a representative animal in Figs 1 and 2, however, the magnitudes of the relative cranial and outward displacements were different depending on the direction of the pull. Specifically, for a given cranial rib displacement, the outward displacement was smaller when the force was applied in the cranial–dorsal than the lateral direction. For a 4 mm cranial rib displacement, for example, the outward rib displacement in the eight animals was 3.90 ± 0.44 mm when the force was applied in the lateral direction, whereas with the force applied in the cranial–dorsal direction, the outward rib displacement was only 2.09 ± 0.19 mm ($P < 0.001$).

Comparison of the rib trajectories produced by ΔP_{di} and external forces

In all animals, the rib trajectory driven by ΔP_{di} lay between the two trajectories produced by external forces in the lateral and the cranial–dorsal direction, as shown in Fig. 2. In six animals, the trajectory driven by ΔP_{di}

was closer to that induced by the external force in the cranial–dorsal direction than to that induced by the external force in the lateral direction, and the vector analysis yields the result that the contribution of the insertional force to the rib displacement driven by ΔP_{di} in the different animals ranged from 43 to 83%. For the animal group, therefore, this contribution amounted to $59.5 \pm 4.4\%$; this value, compared with 50%, was close to the level of statistical significance ($0.05 < P < 0.10$).

Discussion

Three important results were obtained from this study. The first is that the trajectory of lower rib displacement driven by the diaphragm takes place between the trajectories produced by external forces in the cranial–dorsal and lateral directions. This observation supports the conventional wisdom that the force exerted by the diaphragm on the lower ribs has both an insertional component and an appositional component. The second result is that, for a unit pressure, the inspiratory effect of the diaphragm on the lower ribs is equal to the expiratory effect of pleural pressure. The third result is that the insertional force contributes ~60% of that inspiratory effect of the diaphragm, and the appositional force contributes 40%. It should be emphasized that these numbers pertain to the contributions of the two forces to rib displacement, not the relative magnitudes of the forces. In the following paragraphs, we first discuss methodological issues. We then analyse the results of this study and examine the causes of the differences between these results and the estimates previously made by Loring & Mead (1982). Finally, we discuss the implications and limitations of the present observations.

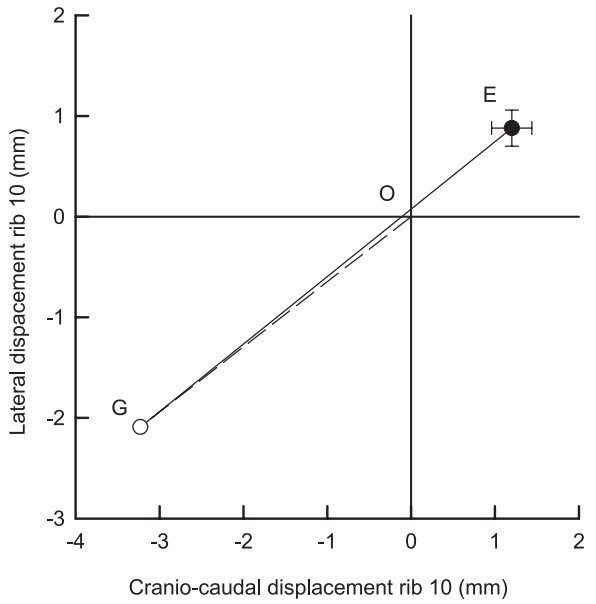

Figure 5. Trajectory of rib displacement produced by pleural and transdiaphragmatic pressure
The filled circle (point E) corresponds to the mean ± SEM rib displacement measured during spontaneous breathing in eight dogs, and the open circle (point G) represents the position of the rib that would have occurred if the change in transdiaphragmatic pressure (ΔP_{di}) were zero. The dashed line O–G, therefore, is the rib displacement produced by the change in pleural pressure (ΔP_{pl}) alone, and the continuous line G–E is the rib displacement due to ΔP_{di} alone. Note that the rib trajectories produced by ΔP_{pl} and ΔP_{di} lie along the same line.

Methodological considerations

In the present experiments, the inspiratory intercostal muscles in all but one interspace were severed. This was essential to achieving the goal of evaluating the effect of the diaphragm. If the intercostals were intact, they would exert an effective inspiratory pressure of unknown magnitude with unknown effects. With the intercostals ineffective, the only forces acting on the ribcage were those generated by ΔP_{pl} and ΔP_{di}, both of which were measured, and the displacements of the ribcage are then functions of these variables. Equations (2) and (3) follow directly from this fact, and the only assumption embodied in these equations is that the relationship between lower rib displacement and ΔP_{pl} and ΔP_{di} is, to a reasonable approximation, a linear relationship. From data for three manoeuvres, the coefficients in these equations were obtained, and these coefficients describe the magnitude of the effects of ΔP_{pl} and ΔP_{di} on lower rib displacement.

Rib displacements were measured along the craniocaudal and laterolateral axes. Displacements in the third dimension, the direction tangent to the arc of the rib, were ignored for three reasons. First, from observations of the constitutive properties of the canine diaphragm and observations of the strain field in the diaphragm *in situ*, Boriek *et al.* (2000) concluded that the muscular portion of the diaphragm carries stress in only one direction, the direction of the muscle bundles. Consequently, the diaphragm exerts only two components of force on the ribcage, the insertional force in the direction of the muscle bundles and the lateral force in the direction perpendicular to the surface of the ribcage. Second, recent measurements using computed tomography showed that during passive, moderate lung inflation, the displacement of rib 10 in the ventral direction is very small compared with the rib displacements in the cranial and lateral directions (Leduc *et al.* 2012). Finally, in preliminary experiments on two animals, it was observed that during isolated diaphragmatic breathing, the lower ribs move cranially and outward, but that their displacement along the ventrodorsal axis is essentially zero.

In order to determine the relative contributions of the two components of the force exerted by the diaphragm on rib 10, external forces were applied to the rib in the craniodorsal and the lateral direction, and the trajectories for these external forces were used as basis vectors for a vector analysis of the rib displacement driven by ΔP_{di}. However, the external forces were applied at a point on a single rib, whereas the forces exerted by ΔP_{di} are distributed around the circumference of the ribcage, and the detailed displacements for the point forces might be different from those for the distributed forces. In fact, the measured displacements for the point forces showed an offset in the lateral displacement at the onset of the force application and then an almost perfectly linear increase with increasing force for cranial displacements in the range from 0.3 to 5.0 mm. The initial lateral displacements were interpreted as being an artifact associated with the point forces, and were neglected. If the initial offsets were included as part of the base displacements for the vector analysis, the calculated contribution of the insertional force would have been slightly greater. Other differences in the displacements of the lower ribs may also have occurred, but the effect of these potential artifacts on the results cannot be assessed.

Effect of diaphragmatic force on the lower ribs

One of the key results of the present study, summarized in eqn (5), is that the net displacement of the lower ribs produced by diaphragmatic contraction is equal to an equivalent of a rib compliance, A, multiplying an effective pressure ($P_{pl} + CP_{di}$). This effective pressure is similar to that previously proposed by Loring & Mead (1982), as shown in eqn (1), ($P_{pl} + BP_{di}$). However, the values obtained in our animals for the coefficient C and for the individual contributions of the appositional and insertional components of ΔP_{di} were very different from the estimates of Loring & Mead (1982) for humans. Thus, the coefficient of ΔP_{di} measured in our animals was approximately 1.0, whereas the estimate of Loring & Mead (1982) was only 0.65. Also, the appositional component of ΔP_{di} in the present study was 0.4, slightly lower than their estimate of 0.5, and the insertional component of ΔP_{di} was 0.6, considerably higher than their estimate of 0.15.

Loring & Mead (1982), however, obtained their estimates from a model of the ribcage, and this model contains the assumption that the ribcage moves as a unit (i.e. with a single degree of freedom). Measurements of thoracoabdominal motion in humans with quadriplegia (Mortola & Sant'Ambrogio, 1978; Danon *et al.* 1979; Strohl *et al.* 1984; Estenne & De Troyer, 1985; Urmey *et al.* 1986) and studies of rib displacement in dogs (De Troyer, 2011, 2012) have shown, however, that this assumption is invalid. Indeed, isolated contraction of the diaphragm during breathing displaces the upper ribs caudally and inward and the lower ribs cranially and outward. Furthermore, Loring & Mead (1982) also assumed that the lower ribs move along a fixed trajectory. In contrast, studies of the action of the canine inspiratory intercostals have subsequently shown that the parasternal intercostals drive the upper ribs cranially and outward, whereas the external intercostals drive these ribs primarily in the cranial direction (De Troyer & Wilson, 2000). In agreement with this finding, the present observations showed that the lower ribs also move with two degrees of freedom and that their trajectory depends on the direction of the forces that are applied to them.

In addition, Loring & Mead (1982) estimated that the contribution of the insertional force to the displacement of the lower ribs was 30% of the contribution of the appositional force, and they described the ratio of the contributions of the two forces as the product of three factors. The first factor was the ratio of the magnitude of the total insertional force to the magnitude of the total appositional force, and they estimated this as the ratio of the cross-sectional area of the thorax to the area of the zone of apposition. Gauthier *et al.* (1994), using computed tomography in normal humans, reported a value of ~0.5 for this ratio. The second factor concerned the distribution of force around the circumference of the diaphragm. Loring & Mead (1982) took this factor to be 0.5 because half of the insertional force acts on the spine and parts of the ribs close to the spine where the force has a small moment around the axis of rib rotation. However, they did not take into account the fact that the appositional force is also distributed around the circumference. As a result of this distribution, the effect of the appositional force would also be expected to be less near the spine. The third factor concerned the angles between the forces and the direction of rib displacement. Loring & Mead (1982) assumed that the angle (φ) between the insertional force and the direction of rib displacement was 60 deg and that the appositional force was aligned with the direction of rib displacement. Thus, the third factor was $\cos \varphi$, and its value was taken as 0.50. However, as shown in Fig. 2, the angle between rib displacement and the cranial direction in our animals was 37 deg. Consequently, the cosine of this angle should be much larger than estimated by Loring & Mead (1982) ($\cos 37 = 0.80$). This angle difference, combined with the distribution of the appositional force, appears to be the major source of the difference between the results of this study and the estimates of Loring & Mead (1982).

Implications and limitations of the study

The results of the present study are significant because, although the data were obtained from manoeuvres in which the diaphragm was the only muscle active during

inspiration, the description of the effect of ΔP_{di} on lower rib displacement applies to any manoeuvre, including normal breathing, in which the intercostal muscles contribute to chest wall expansion. It is worth pointing out, however, that the results pertain to breathing manoeuvres at functional residual capacity. For breathing at higher lung volumes, the area of the zone of apposition would be smaller, so it would be expected that the effect of the appositional force would be smaller and that the value of C in eqn (5) would be <1.0. It is also worth noting that the present results were obtained in dogs and may not apply in detail to humans.

The present results also have two important implications. First, it is well established that, in subjects with quadriplegia, the expansion of the lower portion of the ribcage during inspiration is greater when a passive mechanical support to the abdomen is provided by a pneumatic cuff or an elastic binder (Danon *et al.* 1979; Strohl *et al.* 1984; Urmey *et al.* 1986). This effect is conventionally attributed to an increase in the appositional force of the diaphragm (Strohl *et al.* 1984; Urmey *et al.* 1986). Certainly, when abdominal compliance in quadriplegic subjects is decreased by a pneumatic cuff or a binder, the rise in P_{ab} during inspiration is greater, and the descent of the dome of the diaphragm in response to a given muscle activation is smaller, so that the zone of apposition at end inspiration is larger. However, because a cuff or a binder around the abdomen opposes shortening of the diaphragmatic muscle fibres, it also allows them to operate on a more advantageous portion of their length–tension curve and, thus, to exert greater force on the lower ribs. On the basis of the present observations, one would therefore suggest that the increase in insertional force is likely to play a major role in the greater expansion of the lower ribcage in this setting.

The second implication concerns the contribution to lung volume of the lower rib displacement produced by the diaphragm. In a previous study (De Troyer, 2012), this effect was evaluated by severing all the inspiratory intercostal muscles in dogs and by suppressing the normal inspiratory cranial displacement of the lower ribs produced by spontaneous, isolated diaphragmatic contraction. On the basis of the effect of this procedure, the conclusion was drawn that the lower rib displacement produced by the diaphragm contributed to lung expansion, but that this contribution was only 3–4% of the total ΔP_{pl} generated by the muscle. As shown in Fig. 5, however, the net rib displacement during breathing with the diaphragm alone is small, but the rib displacement driven by the diaphragm is, in fact, much larger. Given that this displacement is approximately four times the net displacement, it follows that the displacement of the lower ribs driven by ΔP_{di} contributes, in fact, up to 12–15% of the total ΔP_{pl}.

References

Baydur A, Bechrakis PK, Zin WA, Jaeger M & Milic-Emili J (1982). A simple method for assessing the validity of the oesophageal balloon technique. *Am Rev Respir Dis* **126**, 788–791.

Boriek AM, Kelly NG, Rodarte JR & Wilson TA (2000). Biaxial constitutive relations for the passive canine diaphragm. *J Appl Physiol* **89**, 2187–2190.

Danon J, Druz WS, Goldberg NB & Sharp JT (1979). Function of the isolated paced diaphragm and the cervical accessory muscles in C1 quadriplegics. *Am Rev Respir Dis* **119**, 909–919.

De Troyer A (2011). The action of the canine diaphragm on the lower ribs depends on activation. *J Appl Physiol* **111**, 1266–1271.

De Troyer A (2012). Respiratory effect of the lower rib displacement produced by the diaphragm. *J Appl Physiol* **112**, 529–534.

De Troyer A & Boriek A (2011). Mechanics of the respiratory muscles. In *Comprehensive Physiology. The Respiratory System: Mechanics of Breathing*, eds. Fredberg J & Sieck G, pp. 1273–1300. Wiley.

De Troyer A & Kelly S (1982). Chest wall mechanics in dogs with acute diaphragm paralysis. *J Appl Physiol* **53**, 373–379.

De Troyer A, Kirkwood PA & Wilson TA (2005). Respiratory action of the intercostal muscles. *Physiol Rev* **85**, 717–756.

De Troyer A, Leduc D, Cappello M & Gevenois PA (2012). Mechanics of the canine diaphragm in pleural effusion. *J Appl Physiol* **113**, 785–790.

De Troyer A & Wilson TA (2000). The canine parasternal and external intercostal muscles drive the ribs differently. *J Physiol* **523**, 799–806.

Estenne M & De Troyer A (1985). Relationship between respiratory muscle electromyogram and rib cage motion in tetraplegia. *Am Rev Respir Dis* **132**, 53–59.

Evans HE & Christensen GC (1979). *Miller's Anatomy of the Dog*, 2nd edn, Saunders, Philadelphia, PA.

Gauthier AP, Verbanck S, Estenne M, Segebarth C, Macklem PT & Paiva M (1994). Three-dimensional reconstruction of the in vivo human diaphragm shape at different lung volumes. *J Appl Physiol* **76**, 495–506.

Leduc D, Cappello M, Gevenois PA & De Troyer A (2012). Mechanism of the lung-deflating action of the canine diaphragm at extreme lung inflation. *J Appl Physiol* **112**, 1311–1316.

Loring SH & Mead J (1982). Action of the diaphragm on the rib cage inferred from a force-balance analysis. *J Appl Physiol* **53**, 756–760.

Mead J (1979). Functional significance of the area of apposition of diaphragm to rib cage. *Am Rev Respir Dis* **119**, 31–32.

Mortola JP & Sant'Ambrogio G (1978). Motion of the rib cage and the abdomen in tetraplegic patients. *Clin Sci Mol Med* **54**, 25–32.

Strohl KP, Mead J, Banzett RB, Lehr J, Loring SH & O'Cain CF (1984). Effect of posture on upper and lower rib cage motion and tidal volume during diaphragm pacing. *Am Rev Respir Dis* **130**, 320–321.

Urmey W, Loring S, Mead J, Slutsky AS, Sarkarati M, Rossier A & Brown R (1986). Upper and lower rib cage deformation during breathing in quadriplegics. *J Appl Physiol* **60**, 618–622.

Additional information

Competing interests

None declared.

Author contributions

A.D. contributed to all aspects of the study. T.A.W. contributed to the study design, data analysis and writing of the manuscript. A.D. and T.A.W. approved the final version of the manuscript.

Funding

This research was supported by a grant from The Brussels School of Medicine.

Acknowledgements

None declared.